Scientific Research Publishing

Open Journal of Orthopedics, 2025, 15(12), 491-506
https://www.scirp.org/journal/ojo
ISSN Online: 2164-3016
ISSN Print: 2164-3008

# Investigation of Bone Union at the Proximal Tibial Osteotomy Site in a Chronic Kidney Disease (CKD) Rat Model

**Kenta Tominaga[1], Yuji Kasukawa[2*], Michio Hongo[3], Koji Nozaka[1], Hiroyuki Nagasawa[1], Hiroyuki Tsuchie[1], Yuichi Ono[1], Manabu Watanabe[1], Takashi Kawaragi[1], Yo Morishita[1], Naohisa Miyakoshi[1]**

[1]Department of Orthopedic Surgery, Akita University Graduate School of Medicine, Akita, Japan
[2]Department of Rehabilitation Medicine, Akita University Hospital, Akita, Japan
[3]Department of Physical Therapy, Akita University Graduate School of Medicine, Akita, Japan
Email: tominaga@med.akita-u.ac.jp, tomikeeeen@gmail.com, *kasukawa@doc.med.akita-u.ac.jp, mhongo@doc.med.akita-u.ac.jp, kk-nozaka@mue.biglobe.ne.jp, nagasawa@med.akita-u.ac.jp, tsuchie@doc.med.akita-u.ac.jp, oyuichi@med.akita-u.ac.jp, kawaragi@med.akita-u.ac.jp, mwatanabe@med.akita-u.ac.jp, ymorishit@med.akita-u.ac.jp, miyakosh@doc.med.akita-u.ac.jp

**How to cite this paper:** Tominaga, K., Kasukawa, Y., Hongo, M., Nozaka, K., Nagasawa, H., Tsuchie, H., Ono, Y., Watanabe, M., Kawaragi, T., Morishita, Y. and Miyakoshi, N. (2025) Investigation of Bone Union at the Proximal Tibial Osteotomy Site in a Chronic Kidney Disease (CKD) Rat Model. *Open Journal of Orthopedics*, **15**, 491-506.
https://doi.org/10.4236/ojo.2025.1512049

**Received:** November 25, 2025
**Accepted:** December 28, 2025
**Published:** December 31, 2025



## Abstract

**Purpose:** Chronic kidney disease (CKD) profoundly affects bone metabolism, contributing to CKD-related mineral and bone disorder and secondary osteoporosis, which increases fracture risk. Delayed bone union is also common in CKD. This study evaluated whether cancellous bone healing at proximal tibial osteotomy sites is delayed in adenine-induced CKD rats. **Methods:** Eight-week-old male Wistar rats were divided into two groups: CKD (fed a 0.75% adenine diet for 4 weeks to induce stage 3 CKD) and control. Proximal tibial osteotomy was performed at age 20 weeks. Bone healing was evaluated at 2 and 4 weeks post-osteotomy via micro-computed tomography (micro-CT) and histological analyses. Serum biochemistry was also assessed. **Results:** CKD rats exhibited significantly elevated blood urea nitrogen and creatinine, indicating renal dysfunction, whereas serum calcium and phosphate remained within normal ranges. Micro-CT analysis showed no significant differences between groups in cortical or trabecular bone parameters at the osteotomy site. However, histological evaluation revealed significantly reduced bone union and cartilage formation in CKD rats 2 weeks post-osteotomy, suggesting delayed early bone healing. By 4 weeks, no significant difference in bone union was observed between groups. Early-stage healing in cancellous bone was delayed in adenine-induced CKD rats, likely due to impaired endochondral ossification. Nevertheless, by 4 weeks post-osteotomy, bone union was comparable in CKD and control rats. **Conclusion:** These findings suggest that CKD,

possibly through disrupted endochondral ossification, transiently delays cancellous bone healing. Further research is warranted to explore potential therapies to enhance fracture healing in CKD.

## Keywords

Chronic Kidney Disease, Bone Healing, Adenine-Induced Model, Tibial Osteotomy, Cancellous Bone, Endochondral Ossification

## 1. Introduction

Chronic kidney disease (CKD) significantly affects bone metabolism due to diminished kidney function. CKD-related mineral and bone disorder and secondary osteoporosis decrease bone strength and markedly increase the risk of fractures in CKD patients [1] [2]. Moreover, fractures in CKD patients are often associated with delayed bone union [3] [4], which prolongs treatment duration and directly shortens healthy life expectancy. CKD also induces systemic abnormalities in bone metabolism, including decreased bone formation, increased bone resorption, and impaired mineralization, which may contribute to delayed bone union. Additionally, CKD patients often exhibit elevated parathyroid hormone (PTH) and fibroblast growth factor 23 (FGF23) levels, which leads to disruption of the normal balance of bone remodeling. These factors suggest that CKD alters the physiology of healing after bone injury [1] [5] [6]. Therefore, reducing fracture risk and promoting bone union when fractures occur are crucial in CKD patients. However, the extent to which CKD delays bone union remains unclear.

Clinical studies of bone union in CKD patients can be challenging due to variability in patient characteristics, the presence of comorbidities, and ethical concerns regarding invasive assessments. Therefore, animal models provide a valuable approach for studying the mechanism of delayed bone union under controlled conditions. Several animal models of CKD have been reported, including the 5/6 nephrectomy model and the adenine-induced CKD model. We previously reported changes in renal function, bone mineral density (BMD), bone microstructure, and skeletal muscle atrophy in adenine-induced CKD model rats. Saito et al. evaluated the stage of CKD by analyzing serum biochemical markers and investigated changes in BMD, bone strength, and bone microarchitecture in adenine-induced CKD model rats [6]. They demonstrated elevated serum creatinine (CRE), phosphorus, and PTH levels, with serum calcium remaining within the normal range, indicative of stage IV CKD accompanied by secondary hyperparathyroidism. Additionally, they observed reduced BMD, deterioration of the cortical bone microstructure, and decreased bone strength in both cortical and cancellous bone [6]. In contrast, Okamoto et al. investigated longitudinal changes in skeletal muscle atrophy in adenine-induced CKD model rats and reported significant muscle weight loss and progressive muscle atrophy associated with the progression of renal dysfunction [7].

Animal fracture models commonly utilize femoral diaphyseal fractures to represent cortical bone fractures; however, we developed a proximal tibial osteotomy model to evaluate bone union specifically in cancellous bone regions. Using this model, we previously reported that pharmacologic treatments and administration of low-intensity pulsed ultrasound promote cancellous bone union. However, whether bone union is delayed in adenine-induced CKD rats after fractures, particularly in cancellous bone regions, remains unclear. Therefore, the purpose of this study was to evaluate the progression of bone union over time at the proximal tibial cancellous bone osteotomy site in adenine-induced CKD model rats.

## 2. Methods

### 2.1. Animal Model and Experimental Design

Eight-week-old, male Wistar rats (N = 40) (Charles River Laboratories Inc., Tokyo, Japan) were housed in a controlled environment (temperature 23˚C ± 2˚C, humidity 40% ± 20%) with a 12-h light-dark cycle and free access to water and rat food. The details were described in a previous report and followed for the selection of rat species and sex [6]. **Figure 1** shows the protocol of this experiment. Rats were classified into the following groups: a control group comprising 20 rats at two time points (n = 10 each at 22 weeks and 24 weeks of age), and a CKD group comprising 20 rats at two time points (n = 10 each at 22 weeks and 24 weeks of age). Animals were monitored daily for general condition and body weight. Humane endpoints were applied when >20% weight loss over 2 - 3 days or severe debilitation was observed. No animals required humane euthanasia, and no unexpected deaths occurred. However, due to rats dying under anesthesia during surgery by respiratory failure (one rat each in the 22 weeks and 24 weeks control groups) and technical errors (one rat each in the 22 weeks and 24 weeks both of control and CKD groups) that occurred during specimen preparation (e.g., section loss, staining defects), samples were analyzed for 8 rats at 22 weeks and 8 rats at 24 weeks in the control group and 9 rats at 22 weeks and 9 rats at 24 weeks in the CKD group.

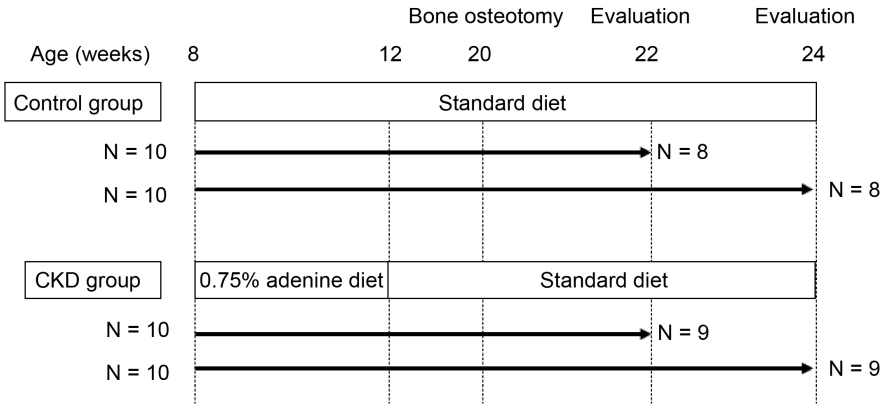


**Figure 1.** Experimental protocol. Cont: non-CKD control rats, CKD: CKD rats.

To generate the CKD model, rats were fed a 0.75% adenine diet (Oriental Yeast Co., Ltd., Tokyo, Japan) for 4 weeks, until 12 weeks of age, followed by a standard rodent chow (CE-7; Clea Japan, Tokyo, Japan). The 4-week adenine diet treatment was selected based on previous studies [6] [8], which reported that 4 weeks of feeding an adenine diet induced non-progressive, irreversible renal failure. Control rats were fed a standard diet without adenine throughout the study.

At 20 weeks of age, all rats underwent proximal tibial osteotomy [9]. **Figure 2** shows a schematic illustration of the osteotomy procedure. Under general anesthesia with isoflurane (2% - 3%), a longitudinal incision was made on the anterior surface of the hind limb to expose the tibia. The tibia was completely transected using a bone saw. The fragments were secured with non-absorbable sutures, and the incision was closed with sutures. The animals were euthanized at 2 and 4 weeks post-osteotomy for evaluation (n = 8~9 in the CKD and control groups at each timepoint). Euthanasia at both 2 and 4 weeks post-osteotomy was performed under 2% - 3% isoflurane inhalation anesthesia followed by blood collection from vena cava, according to the approved protocol.

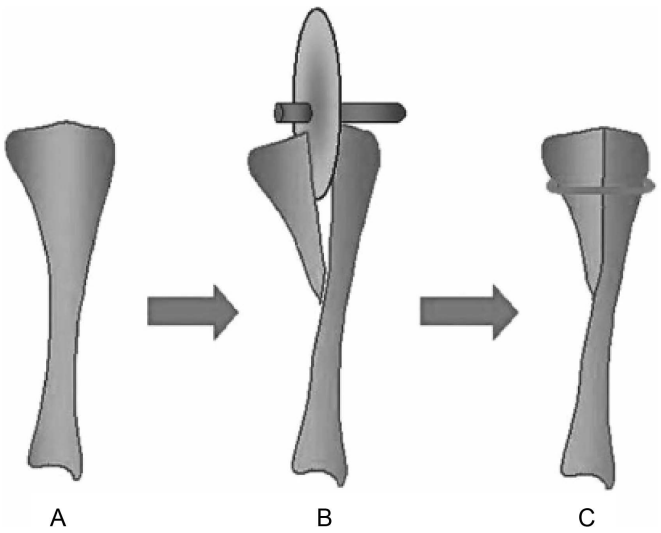


**Figure 2.** Schematic illustration of the surgical procedure of the cancellous bone osteotomy. A complete mid-sagittal osteotomy from the knee joint surface to the tibial outside diaphysis was performed using an electric bone saw (A, B). The fragments were secured with non-absorbable sutures (C).

A post-hoc power analysis was performed for all continuous outcomes. Using the observed effect sizes (Cohen's d) and actual group sizes parse, the post hoc power analysis ($\alpha = 0.05$, two-sided) showed that the number of rats for each group should be 8~9 for the micro-CT and hematoxylin and eosin (H&E) staining analyses. All animal experiments adhered to the protocols approved in advance by the Animal Care and Use Committee of Akita University (approval number a-1-0435, approved on September 12, 2022). Furthermore, all subsequent animal experiments were conducted in accordance with the Animal Care and Use Guide-

lines of our institute.

### 2.2. Body Weight (BW) Measurement

BW was measured weekly from the beginning (20 weeks of age) until the end of the experiment.

### 2.3. Serum Biochemistry Analysis

Blood samples were collected from the vena cava at 2 and 4 weeks post-osteotomy. The collected blood was centrifuged at 3,000 rpm for 30 min at 4˚C to separate the serum, which was aliquoted into disposable tubes and stored at −80˚C until analysis. Blood urea nitrogen (BUN), CRE, calcium (Ca), and inorganic phosphorus (IP) levels were measured using a Fujifilm Dri-Chem 3000V (Fujifilm Corp., Tokyo, Japan).

### 2.4. Micro-CT Analysis

The excised tibia was secured in a specimen holder. Micro-CT imaging was performed using a Cosmo Scan GX II instrument (Rigaku Corp., Tokyo, Japan) according to the manufacturer's instructions. The scanning parameters were set at an isotropic voxel size of 36 μm, voltage of 90 kVp, and current of 88 μA. The acquired images were analyzed using TRI/3D BON software (Ratoc System Engineering Co., Ltd., Tokyo, Japan). The cortical bone area/total bone area ratio (Ct.Ar/Tt.Ar [%]) and cortical thickness (Ct.Th [mm]) were determined to evaluate the cortical bone at the proximal tibial osteotomy site. Trabecular bone was evaluated by determining the bone volume (BV/TV [%]), trabecular thickness (Tb.Th [mm]), trabecular number (Tb.N [/mm]), trabecular separation (Tb.Sp, mm), structure model index (SMI), and degree of anisotropy (DA).

### 2.5. Sample Preparation

After micro-CT imaging, the proximal tibia of each rat was decalcified in 10% neutral ethylenediaminetetraacetic acid for approximately 2 weeks and embedded in paraffin. Mid-frontal slices (thickness: 3 μm) were then sectioned and stained with H&E and Safranin O for cancellous bone histomorphometry. It was difficult to prepare sections appropriate for evaluation for one or two samples in each group or time point. Thus, finally, a total of 8 samples in the control group and 9 samples in the CKD group were examined in micro-CT, bone union, and cartilage formation analyses.

### 2.6. Evaluation of Bone Union after Osteotomy

The rate of bone union was defined as the length of continuous trabecular structure, as measured using ImageJ software [10] [11] on the central slice of coronal sections from both H&E-stained and micro-CT images, divided by the total length of the osteotomy site in the tibia. Cartilaginous bonding was also considered as an indicator of bone union, whereas fibrous bonding was regarded as indicating non-

union. Two authors measured the bone union rate in a blinded fashion. The intraclass correlation coefficient (ICC) measured three times by a single examiner (KT) (ICC 1,3) and ICC measured by two examiner (KT and MW) (ICC 2,2) were as follows: HE staining, 0.999 (ICC 1,3) and 0.980 (ICC 2,2), respectively; and micro-CT, 0.999 (ICC 1,3) and 0.986 (ICC 2,2), respectively.

### 2.7. Evaluation of Bone Formation after Osteotomy

The width of the osteotomy site was defined as the region within which the proximal tibial growth plate was disrupted. The region of interest (ROI) was set as a 1,200 μm × 1,200 μm area, starting 400 μm distal to the growth plate. The bone formation rate was calculated as the area of continuous trabecular structure, excluding fibrous tissue, divided by the total area of the ROI. This ROI was predefined to fully encompass the osteotomy site while ensuring between-specimen reproducibility based on constant anatomical landmarks.

### 2.8. Evaluation of Cartilage Formation after Osteotomy

The rate of cartilage formation was calculated using the same method used to calculate the bone union rate in Safranin O-stained images. Cartilage formation was defined as the length of bone positive for Safranin O staining divided by the length of the osteotomy. The cartilage formation rate was also measured by two authors in a blinded fashion. The ICC (1,3) and ICC (2,2) of cartilage formation were 0.999 and 0.967 respectively.

### 2.9. Statistical Analyses

All data are expressed as the mean ± standard deviation (SD). Data were compared between the control and CKD groups using the Mann-Whitney *U* test. All statistical analyses were performed using EZR [12], which is a modified version of R Commander designed to add statistical functions frequently used in biostatistics. Differences were considered significant at $P < 0.05$.

## 3. Results

### 3.1. BW (Table 1) and Serum Biochemistry (Table 2)

The health status of the animals during the experiment was assessed by measuring the change in BW. At the time of osteotomy (20 weeks of age), the CKD group exhibited significantly lower BW compared to the control group ($P < 0.01$). At 2 weeks post-osteotomy (22 weeks of age), the BW of rats in the CKD group remained significantly lower than that of rats in the control group ($P = 0.035$). However, no significant difference in BW was observed between the two groups at 4 weeks post-osteotomy (24 weeks of age).

Serum biochemistry parameters were analyzed at 2 and 4 weeks post-osteotomy. The results are presented in **Table 2**. At both 2 and 4 weeks post-osteotomy, significant elevations in levels of serum BUN ($P < 0.001$, and $P < 0.001$, respectively) and CRE ($P < 0.001$, and $P < 0.01$, respectively) were observed in the CKD

**Table 1.** Body weight.

| | 20 W | | | 22 W | | | 24 W | | |
|---|---|---|---|---|---|---|---|---|---|
| | Control (n = 20) | CKD (n = 20) | *P*-value vs Control | Control (n = 16) | CKD (n = 18) | *P*-value vs Control | Control (n = 8) | CKD (n = 9) | *P*-value vs Control |
| Body weight (g) | 558.6 ± 35.2 | 503.7 ± 40.4 | <0.001 | 555.2 ± 35.8 | 514.5 ± 43.1 | 0.011 | 570.7 ± 41.3 | 530.4 ± 53.0 | 0167 |

Mann-Whitney *U* test; Values are mean ± standard deviation.

**Table 2.** Serum biochemistry.

| | 22 W | | | 24 W | | |
|---|---|---|---|---|---|---|
| | Control (n = 8) | CKD (n = 9) | *P*-value vs Control | Control (n = 8) | CKD (n = 9) | *P*-value vs Control |
| BUN (mg/dL) | 17.6 ± 2.5 | 34.6 ± 7.9 | <0.001 | 18.5 ± 4.2 | 36.4 ± 8.4 | <0.001 |
| CRE (mg/dL) | 0.17 ± 0.11 | 0.42 ± 0.10 | <0.001 | 0.14 ± 0.12 | 0.46 ± 0.19 | 0.002 |
| Ca (mg/dL) | 12.4 ± 1.3 | 12.2 ± 2.0 | 0.959 | 11.8 ± 1.6 | 11.4 ± 2.5 | 0.673 |
| IP (mg/dL) | 9.8 ± 1.7 | 11.3 ± 3.0 | 0.202 | 11.0 ± 2.7 | 12.1 ± 2.4 | 0.412 |

Mann-Whitney *U* test $P < 0.05$; BUN: blood urea nitrogen, CRE: creatinine, Ca: calcium, IP: inorganic phosphorus.

group compared to the control group, indicating impaired renal function in the CKD rats. No significant differences were observed in serum Ca and serum IP levels between the two groups at 2 and 4 weeks post-osteotomy. The combination of elevated serum creatinine with normal serum calcium and phosphate is characteristic of stage 3 CKD, supporting the validity of the present adenine-induced model.

## 3.2. Micro-CT Analysis of the Osteotomy Site (Table 3)

### 3.2.1. Cortical Bone Evaluation

No significant differences in Ct.Ar/Tt.Ar were observed between the control and CKD groups at 2 and 4 weeks post-osteotomy. Similarly, there were no significant differences in Ct.Th. between the groups at either time point.

### 3.2.2. Trabecular Bone Evaluation

No significant differences in parameters of trabecular bone (BV/TV, Tb.Th, Tb.N, Tb, Sp, SMI, and DA) were observed between the control and CKD groups at 2 and 4 weeks post-osteotomy.

## 3.3. Micro-CT Imaging and Histological Findings at the Osteotomy Site

Although micro-CT demonstrated a gap in the osteotomy site in both the control (**Figure 3(A)**) and CKD (**Figure 3(B)**) groups at 2 weeks, the osteotomy site exhibited bony fusion in the control (**Figure 3(C)**) and CKD (**Figure 3(D)**) groups at 4 weeks post-osteotomy. Micro-CT images showed no significant differences between the control and CKD groups at either 2- or 4-week post-osteotomy.

**Table 3.** Micro-computed tomography at the proximal metaphysis of the tibia.

| | 22 W | | | 24 W | | |
|---|---|---|---|---|---|---|
| | Control (n = 8) | CKD (n = 9) | *P*-value vs Control | Control (n = 8) | CKD (n = 9) | *P*-value vs Control |
| Cortical bone | | | | | | |
| Ct.Ar/Tt.Ar (%) | 48.1 ± 6.2 | 45.1 ± 4.5 | 0.541 | 41.4 ± 4.2 | 38.0 ± 9.2 | 0.423 |
| Ct.Th (μm) | 333.2 ± 93.5 | 289.8 ± 84.5 | 0.541 | 449.0 ± 169.1 | 389.2 ± 199.3 | 0.277 |
| Trabecular bone | | | | | | |
| BV/TV (%) | 41.2 ± 12.0 | 40.7 ± 10.2 | 0.851 | 24.8 ± 12.3 | 36.8 ± 13.6 | 0.114 |
| Tb.Th (μm) | 34.1 ± 8.5 | 32.3 ± 5.8 | 1 | 27.1 ± 3.9 | 31.7 ± 6.2 | 0.167 |
| Tb.N (1/mm) | 1.2 ± 0.1 | 1.3 ± 0.2 | 0.888 | 0.9 ± 0.3 | 1.1 ± 0.3 | 0.167 |
| Tb.Sp (μm) | 504.2 ± 152.5 | 491.0 ± 133.5 | 0.963 | 1015.0 ± 468.5 | 669.7 ± 462.1 | 0.139 |
| SMI | 0.9 ± 0.6 | 1.2 ± 0.6 | 0.673 | 2.0 ± 0.8 | 1.3 ± 0.9 | 0.075 |
| DA | 1.5 ± 0.1 | 1.5 ± 0.2 | 0.321 | 1.6 ± 0.2 | 1.6 ± 0.2 | 0.423 |

Mann-Whitney *U* test $P < 0.05$; Values are mean ± standard deviation; Ct.Ar/Tt.Ar: cortical area/total area, Ct.Th: cortical thickness, BV/TV: bone volume/tissue volume, Tb.Th: trabecular thickness, Tb.N: trabecular number, Tb.Sp: trabecular separation, SMI: structure model index, DA: degree of anisotropy.

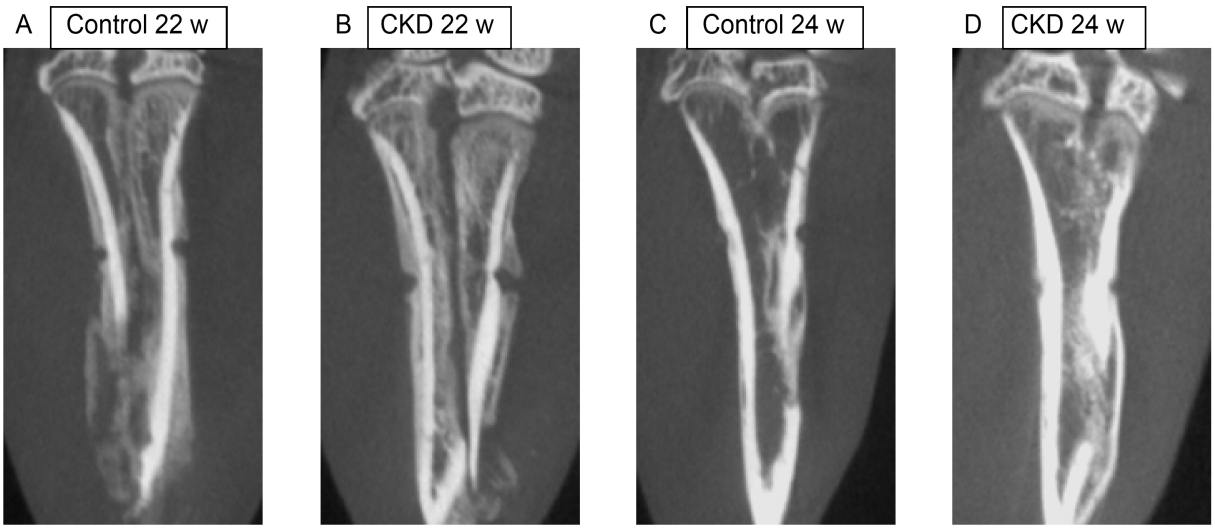


**Figure 3.** Micro-CT images, central slice of coronal sections, showed no significant differences between the control (A and C, respectively) and CKD (B and D, respectively) groups at both 2 and 4 weeks post-osteotomy.

At 2 weeks post-osteotomy, most areas of the osteotomy site in both the control and CKD groups were filled with fibrous tissue (**Figure 4(A)** and **Figure 4(B)**) in H&E-stained sections. By 4 weeks post-osteotomy, both groups demonstrated thick trabecular bone and dense bone union at the osteotomy site (**Figure 4(C)** and **Figure 4(D)**).

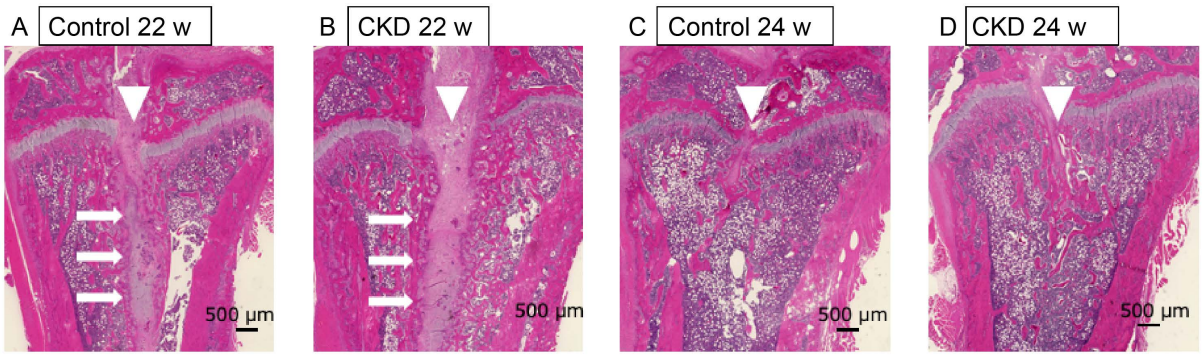


**Figure 4.** Histological sections of the osteotomy site stained with hematoxylin and eosin. Arrowheads (▽) indicate sites of interruption of the growth plate. At 2 weeks post-osteotomy, most of the areas at the osteotomy site were filled with fibrous tissues (arrows) in both the control (A) and CKD (B) groups. At 4 weeks post-osteotomy, both the control (C) and CKD (D) groups demonstrated thick trabecular bone and dense bone union at the osteotomy site.

## 3.4. Rates of Bone Union and Bone Formation at the Osteotomy Site (Table 4)

### 3.4.1. Bone Union Rate at the Osteotomy Site

Bone union rates were assessed using micro-CT and showed no significant differences between the control and CKD groups at either the 2- or 4-week post-osteotomy time points. Bone union rates, as assessed using H&E-stained sections, were significantly lower in the CKD group at 2 weeks post-osteotomy compared to the control group ($P = 0.048$). However, at 4 weeks post-osteotomy, no significant differences were observed between the control and CKD groups.

**Table 4.** Bone union/formation rates.

| | 22 W | | | 24 W | | |
|---|---|---|---|---|---|---|
| | Control (n = 8) | CKD (n = 9) | *P*-value vs Control | Control (n = 8) | CKD (n = 9) | *P*-value vs Control |
| Bone union rate (%) | | | | | | |
| Micro-CT | 37.7 ± 18.9 | 32.7 ± 25.0 | 0.370 | 97.7 ± 4.0 | 90.8 ± 10.3 | 0.086 |
| H&E-stained section | 29.3 ± 17.7 | 15.8 ± 18.8 | 0.048 | 83.4 ± 17.2 | 68.3 ± 22.1 | 0.160 |
| Bone formation rate (%) | 50.9 ± 21.3 | 47.6 ± 19.9 | 0.673 | 96.8 ± 3.4 | 86.1 ± 15.3 | 0.311 |

Mann-Whitney U test $P < 0.05$; Values are mean ± standard deviation. H&E: hematoxylin and eosin.

### 3.4.2. Bone Formation Rate at the Osteotomy Site

Bone formation rates assessed by H&E staining showed no significant differences between the control and CKD groups at both 2 and 4 weeks post-osteotomy.

## 3.5. Cartilage Formation at the Osteotomy Site

Figure 5 shows histological sections of the osteotomy site stained with Safranin O. At 2 weeks post-osteotomy, cartilage formation was observed at the osteotomy site in the control group (Figure 5(A)), but not in the CKD group (Figure 5(B)). After 4 weeks, no cartilage formation was observed in either the control (Figure

5(C)) or CKD (Figure 5(D)) group. Cartilage formation rates assessed by Safranin O staining were significantly lower in the CKD group than in the control group at 2 weeks post-osteotomy ($P = 0.017$) (Table 5). However, no significant differences were observed between the control and CKD groups at 4 weeks post-osteotomy (Table 5).

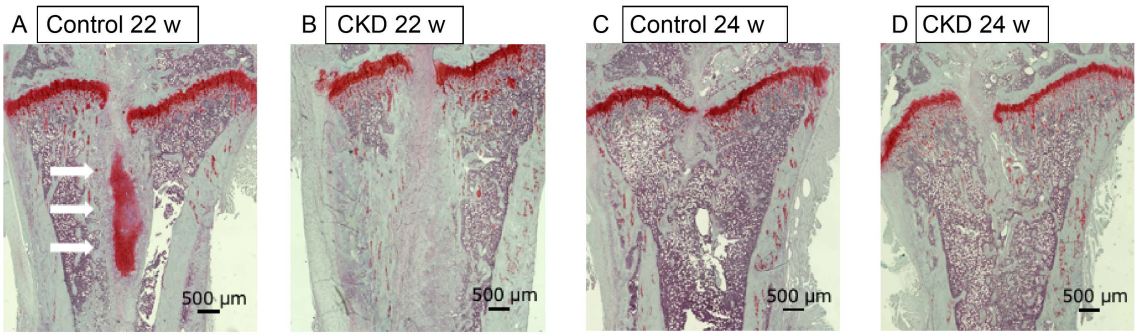


Figure 5. Histological sections of the osteotomy site stained with Safranin O. Cartilage formation was observed at 2 weeks post-osteotomy in the control (A) group (arrows), and the rate of cartilage formation was lower in the CKD group (B) than in the control group (A). No significant changes between the control (C) and CKD (D) groups were observed at 4 weeks post-osteotomy.

Table 5. Cartilage formation rate.

| | 22 W | | | 24 W | | |
|---|---|---|---|---|---|---|
| | Control (n = 8) | CKD (n = 9) | *P*-value vs Control | Control (n = 8) | CKD (n = 9) | *P*-value vs Control |
| Cartilage formation rate (%) | 23.4 ± 5.0 | 8.4 ± 11.6 | 0.017 | 0.8 ± 2.0 | 0.0 ± 0.0 | 0.346 |

Mann-Whitney U test $P < 0.05$; Values are mean ± standard deviation.

## 4. Discussion

### 4.1. Summary of the Present Study

In this study, we used a rat model of adenine-induced CKD to evaluate whether prolonged bone healing occurs at the osteotomy site of the proximal tibia. Serological examinations confirmed that the model rats had stage 3 CKD, as serum CRE was elevated and Ca and IP were within the normal range. Micro-CT analysis showed no difference in the bone healing rate of the proximal tibial cancellous osteotomy between the control and CKD rats and no evidence of prolonged bone healing. However, bone tissue specimens showed a significant decrease in the rate of bone healing and cartilage formation in CKD rats at a relatively early stage of 2 weeks post-osteotomy. In contrast, there was no difference in bone healing rate at 4 weeks, which was later after osteotomy. The bone microstructure of the proximal tibial osteotomy showed no deterioration of either cortical or trabecular bone parameters in CKD rats. In conclusion, in the adenine-induced CKD rat model, bone healing of the proximal tibial cancellous bone osteotomy was prolonged in the early-stage post-osteotomy due to histologically delayed endochondral ossifi-

cation, but histological analyses did not indicate prolonged healing at 4 weeks post-osteotomy.

### 4.2. Delay in Bone Union and Its Mechanism in CKD

CKD severely affects bone metabolism, resulting in decreased bone formation, increased bone resorption, and abnormal mineral metabolism [1]. These changes increase the risk of fracture in patients with CKD and are likely to result in prolonged bone healing after fracture. Indeed, in clinical practice, fractures are observed more frequently in CKD patients with a low estimated glomerular filtration rate [13], and an increased risk of hip fracture in these patients has also been reported [14]. In a clinical study of 130 patients with femoral neck fractures, those with CKD had a higher risk of pseudoarthrosis than those with normal renal function [4], and pseudoarthrosis of distal femur fractures in patients with renal osteodystrophy due to CKD has been reported [3]. Therefore, renal impairment may prolong bone healing or increase the risk of pseudoarthrosis. Animal studies have shown that CKD reduces BMD and negatively impacts the bone microstructure and bone strength [6] [15] [16]. Bone regeneration capacity is reportedly reduced with respect to bone healing in CKD models involving artificially created bone defects [17].

### 4.3. Possible Mechanisms of Delayed Cancellous Bone Healing

In this study, delayed bone healing was observed in the CKD group, especially in the early period post-osteotomy. Possible mechanisms for this delay include the following. Serum BUN and CRE levels were significantly higher in the CKD group than in the control group in this study, suggesting that the CKD was stage 3. This degree of renal dysfunction may have affected bone formation. Both bone resorption and bone formation are stimulated in adenine-induced CKD model rats, resulting in high bone metabolic turnover [6], which in turn leads to bone loss and bone fragility [6] [16] [18]. CKD also causes secondary hyperparathyroidism, which increases the number of osteoclasts and osteoblasts [17]. In our previous study, intact PTH levels were significantly higher in CKD rats aged 12 to 20 weeks than in control rats [6] under the same conditions to which the adenine-induced CKD model rats in this study were subjected. Because the same adenine-induced CKD protocol was used in this study, the markedly elevated PTH levels indicate the presence of secondary hyperparathyroidism in the current model as well, strengthening the interpretation that altered hormonal conditions contributed to delayed endochondral ossification. Therefore, secondary hyperparathyroidism may have also played a role in prolonged bone healing. Furthermore, FGF23 levels are elevated in CKD, which reportedly leads to decreased vitamin D receptor (VDR) expression, suggesting that decreased VDR expression may inhibit osteoblast differentiation and reduce osteogenic potential [19].

### 4.4. Relationship between Bone Union and Cartilage Formation

Previous studies have reported that CKD causes impaired endochondral ossifica-

tion and growth retardation; in CKD model rats, the structure of the growth chondrocyte plate was disrupted, and the normal arrangement of chondrocytes was impaired. In particular, the height of mature hypertrophic chondrocytes was reduced, and the cell maturation process was disrupted. The proliferation rate of cells was also reduced in the growing chondrocyte version of the CKD rat model. The distribution of osteoclasts was also uneven, and their number was increased, resulting in an impairment of the trabecular bone microstructure. Furthermore, it has been reported that secondary hyperparathyroidism interferes with osteogenesis and calcification processes and inhibits the process of endochondral ossification [20]. The above factors may have delayed endochondral ossification and reduced the rate of early bone healing and cartilage formation. CKD also leads to decreased expression of vascular endothelial growth factor (VEGF), which is essential for angiogenesis and endochondral ossification in fracture healing. However, when VEGF expression is reduced due to CKD, vascular invasion into the fracture site is delayed, leading to pseudostratified bone. However, another study reported that when VEGF is decreased due to CKD, both vascular invasion into the fracture site and ossification of pseudo-bone are delayed [21]. In the present study, CKD may have caused impaired endochondral ossification and prolonged bone healing. In this study, VEGF immunostaining did not yield detectable signals. This was likely due to technical limitations associated with hard-tissue processing, including prolonged decalcification, which can reduce antigenicity. In addition, previous studies have reported decreased VEGF expression in CKD, which may have further contributed to the weak staining observed. The delayed cartilage maturation observed in CKD rats was evident in the Safranin O-stained sections in **Figure 5**, where persistent cartilaginous tissue and immature matrix were present at the osteotomy site compared with the controls. These findings support the interpretation of delayed endochondral ossification in the CKD group.

### 4.5. Micro-CT versus Histology

Notably, radiographic bone-bridging on micro-CT did not always correspond to histological union. A known limitation of micro-CT is its inability to distinguish mature lamellar bone from newly mineralized woven bone or cartilage. Therefore, micro-CT may overestimate apparent bony continuity compared with histology, which directly reflects tissue maturity. This discrepancy reflects methodological differences: micro-CT primarily captures the continuity of mineralized tissue and is affected by thresholding and spatial resolution, whereas histology reveals residual cartilage and tissue maturity at the osteotomy site. Thus, apparent bridging on micro-CT may precede the completion of endochondral ossification on histology, particularly under CKD conditions. Prior studies have implicated cyclin-dependent kinase 1 (Cdk1) in osteoblast proliferation and bone formation. Loss of Cdk1 impairs bone formation without abolishing the anabolic effects of PTH [22], and disease-related tissue changes can involve altered Cdk1-related pathways [23]. Although we did not assess Cdk1 in this study, the delayed endochondral matu-

ration observed in CKD could be somewhat consistent with cell cycle-linked dysregulation. However, the present study focuses on phenotypic/histological findings, thus molecular-level mechanisms are speculative. Future work should examine Cdk1 expression and signaling in CKD-associated delayed union.

### 4.6. Limitations

First, in this study, bone union was evaluated at 2 and 4 weeks post-osteotomy, but bone fusion was already complete at 4 weeks. Earlier observations, such as at 1-week post-osteotomy, could be necessary. Second, the detailed analysis of abnormalities in bone metabolism was insufficient because serum PTH and FGF23 levels were not measured. However, the model used in this study was the same as that used in a previous study [6], in which serum PTH was elevated, suggesting secondary hyperparathyroidism. In the future, we plan to investigate the possibility of promoting bone healing in CKD patients by combining drug administration and low-power ultrasound pulses. Third, the study examined a relatively low number of rats, even though the post hoc power analysis indicated the inclusion of 8~9 rats for micro-CT analysis and H&E staining in each group. Thus, it was not possible to completely avoid the risk of type II errors in this exploratory study. Finally, we did not perform a dynamic bone histomorphometry and evaluation of Osteoprotegerin/receptor activator of nuclear factor-kappa B ligand due to limited available resources. An evaluation of bone metabolic markers would be needed in future study.

## 5. Conclusion

This study demonstrated that bone healing and cartilage formation are suppressed in a rat model of CKD, particularly in the early post-osteotomy period. The results suggest that renal dysfunction, secondary hyperparathyroidism, and impaired endochondral ossification are involved in the mechanism of delayed bone healing due to CKD. These findings highlight a clinically important early post-fracture period during which patients with CKD may be particularly vulnerable to impaired healing, underscoring the need for careful postoperative monitoring and consideration of early therapeutic strategies. Further investigation of treatment strategies designed to promote bone healing is needed.

## Ethics Approval and Consent to Participate

All animal experiments adhered to the protocols approved in advance by the Animal Care and Use Committee of our institute (approval number a-1-0435, approved on September 12, 2022). Furthermore, all subsequent animal experiments were conducted in accordance with the Animal Care and Use Guidelines of our institute.

## Patient Consent for Publication

Not applicable.

## Availability of Data and Materials

The datasets generated and/or analyzed during the current study are available from the corresponding author upon reasonable request.

## Authors' Contributions

**Kenta Tominaga**: Investigation, Validation, Visualization, Writing—Original Draft.

**Yuji Kasukawa**: Conceptualization, Methodology, Project Administration, Writing—Review & Editing. **Michio Hongo**: Conceptualization, Methodology, Writing—Review & Editing. **Koji Nozaka**: Conceptualization, Methodology, Writing—Review & Editing. **Hiroyuki Nagasawa**: Investigation, Formal Analysis. **Hiroyuki Tsuchie**: Investigation, Formal Analysis. **Yuichi Ono**: Investigation. **Manabu Watanabe**: Investigation. **Takashi Kawaragi**: Investigation. **Yo Morishita**: Investigation. **Naohisa Miyakoshi**: Conceptualization, Funding Acquisition, Supervision, Writing—Review & Editing.

## Acknowledgements

The authors would like to thank Ms. Midorikawa for her support of our experiments and FORTE Science Communications for English language editing.

## Use of Artificial Intelligence Tools

Artificial intelligence tools were used only to support translation and grammar correction in the preparation of the manuscript. The authors take full responsibility for the content and integrity of the manuscript.

## Conflicts of Interest

The authors declare that they have no competing interests.

## References

[1] Pazianas, M. and Miller, P.D. (2021) Osteoporosis and Chronic Kidney Disease-Mineral and Bone Disorder (CKD-MBD): Back to Basics. *American Journal of Kidney Diseases*, **78**, 582-589. https://doi.org/10.1053/j.ajkd.2020.12.024

[2] Nickolas, T.L., McMahon, D.J. and Shane, E. (2006) Relationship between Moderate to Severe Kidney Disease and Hip Fracture in the United States. *Journal of the American Society of Nephrology*, **17**, 3223-3232. https://doi.org/10.1681/asn.2005111194

[3] Jin, H., Xiong, M., Zhou, H., Zhang, M., He, X. and Pu, D. (2020) Use of a Titanium Cage and Intramedullary Nails to Treat Distal Femoral Fracture Nonunion in a Patient with Renal Osteopathy: A Case Report. *American Journal of Case Reports*, **21**, e924565. https://doi.org/10.12659/ajcr.924565

[4] Kuo, L., Lin, S., Hsu, W., Peng, K., Lin, C. and Hsu, R.W. (2013) The Effect of Renal Function on Surgical Outcomes of Intracapsular Hip Fractures with Osteosynthesis. *Archives of Orthopaedic and Trauma Surgery*, **134**, 39-45. https://doi.org/10.1007/s00402-013-1884-5

[5] Isakova, T., Wahl, P., Vargas, G.S., Gutiérrez, O.M., Scialla, J., Xie, H., *et al.* (2011)

Fibroblast Growth Factor 23 Is Elevated before Parathyroid Hormone and Phosphate in Chronic Kidney Disease. *Kidney International*, **79**, 1370-1378. https://doi.org/10.1038/ki.2011.47

[6] Saito, H., Miyakoshi, N., Kasukawa, Y., Nozaka, K., Tsuchie, H., Sato, C., *et al.* (2021) Analysis of Bone in Adenine-Induced Chronic Kidney Disease Model Rats. *Osteoporosis and Sarcopenia*, **7**, 121-126. https://doi.org/10.1016/j.afos.2021.11.001

[7] Okamoto, K., Kasukawa, Y., Nozaka, K., Tsuchie, H., Kudo, D., Kinoshita, H., *et al.* (2024) Changes in Skeletal Muscle Atrophy over Time in a Rat Model of Adenine-Induced Chronic Kidney Disease. *Applied Sciences*, **14**, Article 9106. https://doi.org/10.3390/app14199106

[8] Igarashi, S., Kasukawa, Y., Nozaka, K., Tsuchie, H., Abe, K., Saito, H., *et al.* (2023) Teriparatide and Etelcalcetide Improve Bone, Fibrosis, and Fat Parameters in Chronic Kidney Disease Model Rats. *Osteoporosis and Sarcopenia*, **9**, 121-130. https://doi.org/10.1016/j.afos.2023.11.002

[9] Tsuchie, H., Miyakoshi, N., Kasukawa, Y., Aonuma, H. and Shimada, Y. (2013) Intermittent Administration of Human Parathyroid Hormone before Osteosynthesis Stimulates Cancellous Bone Union in Ovariectomized Rats. *The Tohoku Journal of Experimental Medicine*, **229**, 19-28. https://doi.org/10.1620/tjem.229.19

[10] Abramoff, M.D., Magelhaes, P.J. and Ram, S.J. (2003) Image Processing with ImageJ. *Biophotonics International*, **11**, 36-42.

[11] Schneider, C.A., Rasband, W.S. and Eliceiri, K.W. (2012) NIH Image to ImageJ: 25 Years of Image Analysis. *Nature Methods*, **9**, 671-675. https://doi.org/10.1038/nmeth.2089

[12] Kanda, Y. (2012) Investigation of the Freely Available Easy-To-Use Software 'EZR' for Medical Statistics. *Bone Marrow Transplantation*, **48**, 452-458. https://doi.org/10.1038/bmt.2012.244

[13] Naylor, K.L., McArthur, E., Leslie, W.D., Fraser, L., Jamal, S.A., Cadarette, S.M., *et al.* (2014) The Three-Year Incidence of Fracture in Chronic Kidney Disease. *Kidney International*, **86**, 810-818. https://doi.org/10.1038/ki.2013.547

[14] Tang, C. and Chou, C. (2021) Hip Fracture in Patients with Non-Dialysis Chronic Kidney Disease Stage 5. *Scientific Reports*, **11**, Article No. 20591. https://doi.org/10.1038/s41598-021-00157-1

[15] Bajwa, N.M., Sanchez, C.P., Lindsey, R.C., Watt, H. and Mohan, S. (2018) Cortical and Trabecular Bone Are Equally Affected in Rats with Renal Failure and Secondary Hyperparathyroidism. *BMC Nephrology*, **19**, Article No. 24. https://doi.org/10.1186/s12882-018-0822-8

[16] Ni, L., Tang, R., Lv, L., Wu, M., Wang, B., Wang, F., *et al.* (2018) A Rat Model of SHPT with Bone Abnormalities in CKD Induced by Adenine and a High Phosphorus Diet. *Biochemical and Biophysical Research Communications*, **498**, 654-659. https://doi.org/10.1016/j.bbrc.2018.03.038

[17] Liu, W., Kang, N., Seriwatanachai, D., Dong, Y., Zhou, L., Lin, Y., *et al.* (2016) Chronic Kidney Disease Impairs Bone Defect Healing in Rats. *Scientific Reports*, **6**, Article No. 23041. https://doi.org/10.1038/srep23041

[18] Hu, T., Chen, J., Shao, S., Li, L., Lai, C., Gao, W., *et al.* (2023) Biomechanical and Histomorphological Analysis of the Mandible in Rats with Chronic Kidney Disease. *Scientific Reports*, **13**, Article No. 21886. https://doi.org/10.1038/s41598-023-49152-8

[19] Zhou, S. and Glowacki, J. (2017) Chronic Kidney Disease and Vitamin D Metabolism

in Human Bone Marrow-Derived MSCs. *Annals of the New York Academy of Sciences*, **1402**, 43-55. https://doi.org/10.1111/nyas.13464

[20] Claramunt, D., Gil-Peña, H., Fuente, R., García-López, E., Loredo, V., Hernández-Frías, O., *et al.* (2015) Chronic Kidney Disease Induced by Adenine: A Suitable Model of Growth Retardation in Uremia. *American Journal of Physiology-Renal Physiology*, **309**, F57-F62. https://doi.org/10.1152/ajprenal.00051.2015

[21] Troib, A., Landau, D., Kachko, L., Rabkin, R. and Segev, Y. (2013) Epiphyseal Growth Plate Growth Hormone Receptor Signaling Is Decreased in Chronic Kidney Disease-Related Growth Retardation. *Kidney International*, **84**, 940-949. https://doi.org/10.1038/ki.2013.196

[22] Takahashi, A., Mulati, M., Saito, M., Numata, H., Kobayashi, Y., Ochi, H., *et al.* (2018) Loss of Cyclin-Dependent Kinase 1 Impairs Bone Formation, but Does Not Affect the Bone-Anabolic Effects of Parathyroid Hormone. *Journal of Biological Chemistry*, **293**, 19387-19399. https://doi.org/10.1074/jbc.ra118.004834

[23] Li, C., Peng, Z., Zhou, Y., Su, Y., Bu, P., Meng, X., *et al.* (2021) Comprehensive Analysis of Pathological Changes in Hip Joint Capsule of Patients with Developmental Dysplasia of the Hip. *Bone & Joint Research*, **10**, 558-570. https://doi.org/10.1302/2046-3758.109.bjr-2020-0421.r2